Письма в ЭЧАЯ. 2015. Т. 12, № 2(193). С. 299–312

REMARKS ON SIMPLE MODIFIED PERTURBATION THEORY

D. V. Shirkov [1]

Joint Institute for Nuclear Research, Dubna

The goal is to devise a pQCD modification that should be regular in the low-energy region and could serve practically for the data analysis below 1 GeV up to the infra-red limit. The recently observed "blow-up" of the 4-loop pQCD series for the Bjorken sum rule form factor around $Q \lesssim 1$ GeV and partial resolving of the issue with the help of the Analytic Perturbation Theory (APT) until $Q \sim 0.6$ GeV provided the impetus for this attempt.

The "massive pQCD" under construction has two grounds. The first is pQCD with only one parameter added, an effective "glueball mass" $m_\rho \lesssim M_{\rm glb} \lesssim 1$ GeV, serving as an infra-red regulator. Roughly, we introduce it by changing the ultra-violet $\ln Q^2$ for a massive log, $\ln\left(Q^2 + M^2_{\rm glb}\right)$ regular in the low-energy region and finite in the infra-red limit. The second stems from the ghost-free APT comprising non-power perturbative expansion that makes it compatible with linear integral transformations.

Предложена модификация теории возмущений для квантовой хромодинамики (pQCD), регулярная в области низких энергий и дающая практический метод анализа данных ниже 1 ГэВ вплоть до инфракрасной границы. Импульсом для этой попытки послужили недавно открытый рост pQCD-рядов начиная с 4-петель для правил сумм Бьеркена при $Q \lesssim 1$ ГэВ и частичное решение проблемы при помощи аналитической теории возмущений (АТВ) вплоть до $Q \sim 0{,}6$ ГэВ.

Рассматриваемая «массивная pQCD» имеет два основания. Первое состоит в том, что к pQCD добавляется только один новый параметр — эффективная «масса глюбола» $m_\rho \lesssim M_{\rm glb} \lesssim 1$ ГэВ, которая является инфракрасным регулятором. Грубо говоря, мы вводим ее, заменяя ультрафиолетовые логарифмы $\ln Q^2$ массивным, $\ln\left(Q^2 + M^2_{\rm glb}\right)$, который регулярен в области низких энергий и конечен в инфракрасном пределе. Второе основание связано со свободной от духов и нестепенной АТВ. Это делает теорию возмущений совместимой с линейными интегральными преобразованиями.

PACS: 11.10.Jj; 11.15.Tk; 12.38.Aw

1. INTRODUCTION: MOTIVATION AND OUTLINE

The perturbative QCD (pQCD) [2] is a firmly established part of particle interaction theory. Starting with gauge-non-invariant quantization, it correlates several dozens of experiments at quite different scales from a few up to hundreds of GeV. At the same time, pQCD meets troubles in the low-energy (large-distance) domain, below a few GeV, at the scales marked by the QCD parameter $\Lambda \lesssim 380$ MeV. This Achilles' heel is related to its ultra-violet origin essence.

[1] E-mail: mikhs@theor.jinr.ru

[2] The renormalization group improved QCD perturbation expansion *taken in the ultra-violet limit.*

To avoid the unwanted singularity in the low-energy region, several modifications [1–5] of the pQCD have been devised. Recently, one of them, the Analytic Perturbation Theory (APT) ([6, 7] and a later review paper [8]), has proved to be good [9] in describing the polarized $\Gamma_1^{p-n}(Q^2) = \Gamma_1(Q^2)$ form factor of the Bjorken Sum Rules (BjSR) amplitude *down to a few hundred MeV*.

The difference of proton and neutron Bjorken moments is usually presented as a sum of perturbation theory (PT) and higher twist (HT) non-perturbative contributions:

$$\Gamma_1(Q^2) = \frac{g_A}{6}\left[1 - \Delta_{\rm Bj}^{\rm PT}(Q^2)\right] + \Gamma_{\rm HT}, \quad \Gamma_{\rm HT} = \sum_{i=2}^{\infty} \frac{\mu_{2i}}{Q^{2i-2}}, \tag{1}$$

with $\Delta_{\rm Bj}^{\rm PT}$, including the $N^3LO \sim (\alpha_s(Q^2))^4$ term. However, an attempt to fit rather precise JLab data by expression (1) with appropriate higher twist coefficients failed as the perturbation theory part exploded (Fig. 1) in the region 0.7–1 GeV and the extracted (via comparison with fitted JLab data) μ_{2i} values turned out to be unstable with respect to higher loop terms in the first perturbation theory sum. This prevented data description below 1 GeV (Fig. 2). Along with Eq. (1), in [9] the perturbation theory sum was changed for the APT one [1]:

$$\Delta_{\rm Bj}^{\rm PT}(Q^2) = \sum_{k\leqslant 4} c_k (\alpha_s(Q^2))^k \Rightarrow \Delta_{\rm Bj}^{\rm APT}(Q^2) = \sum_{k\leqslant 4} c_k\, A_k(Q^2), \tag{2}$$

where $A_k(Q^2)$ is the APT [6, 7] ghost-free expansion functions. The change resulted in good fitting of the JLab data down to a few hundred MeV (Fig. 2) with stable higher twist parameters.

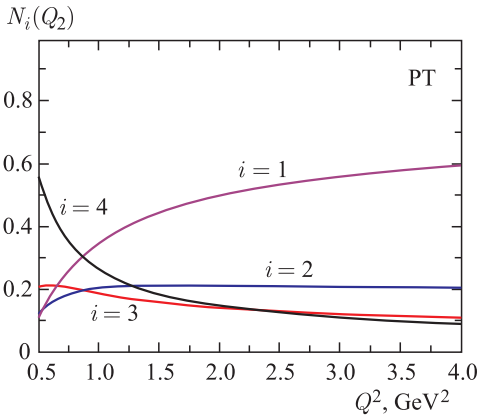

Fig. 1. Relative contributions N_i of perturbation theory terms to $\Delta_{\rm Bj}^{\rm PT}(Q^2)$

This result begets hope for the global fitting down to the infra-red limit. Unfortunately, none of the above-mentioned ghost-free modifications [1–5] is suitable for this purpose. The common drawback is the use of ultra-violet logs in the infra-red region.

To approach the global fitting of data (like these for the BjSR form factor), one needs a modified perturbation theory (MPT) with two essential properties:

- correspondence with common pQCD in ultra-violet limit (that is above a few GeV);
- regularity and finiteness of the modified effective coupling $\alpha_s^{\rm MPT}(Q)$ and matrix elements in the low-energy domain.

As a primary launch pad for this construction, the above-mentioned APT seems good. It satisfies the first condition and, partially, the second one. To exempt the APT-like scheme from its last drawback — the singularity (infinite derivatives) in the infra-red limit, one has to disentangle it from the ultra-violet logs.

[1] In the current paper, we change the original notation $\mathcal{A}_k$ for the A_k one.

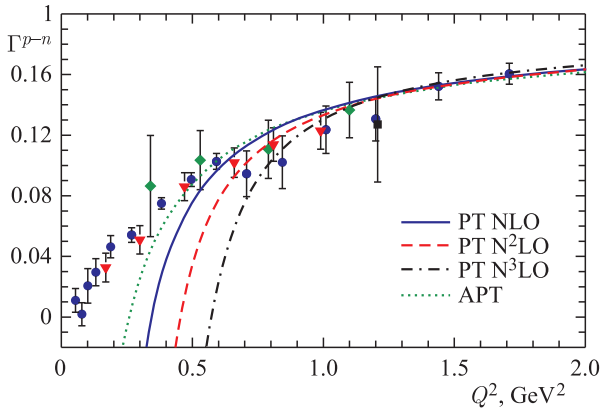

Fig. 2. The pQCD anti-progress below $Q < 1$ GeV as $2 \to 3 \to 4$-loops

For this purpose, in the first version of this research [10], the infra-red regulator has been introduced just by the shift of the Q^2 scale,

$$Q^2 \to Q^2 + M^2_{\rm glb} \tag{3}$$

with the only fitting parameter added, an effective glueball mass $M_{\rm glb}$.

Here, we are going to address one more trick evoked by unitarity [11, 12] arguments [1]:

$$\ln x \to J(x) = 2\sqrt{\frac{x+1}{x}}\,\text{arctanh}\left[\left(\frac{x}{1+x}\right)^{1/2}\right] = 2\sqrt{\frac{x+1}{x}}\ln\left(\sqrt{x}+\sqrt{x+1}\right),$$

where $x \equiv Q^2/M^2_{\rm glb}$. This "quasi-rapidity" $J(x)$ tends to the usual ultra-violet log at high $Q^2 \gg M^2_{\rm glb}$,

$$J(x \gg 1) = \ln x + 2\,\ln 2 + \frac{1}{2x}\ln x, \tag{4}$$

and behaves as

$$J(x \ll 1) = 2 + \frac{2}{3}x - \frac{4}{15}x^2, \tag{5}$$

in the infra-red limit.

2. GENERAL RELATIONS

2.1. Two-Loop Massive Renormalization Group Solution. At low energy (below m_τ) we use the two-loop massive renormalization group solution in the denominator representation [2] (see [14])

$$\mathcal{A}_1(x) = \mathsf{a}(\phi) = \frac{\alpha_0}{1 + \alpha_0\beta_0\phi + \alpha_0\, b\,\ln\left(1 + \alpha_0\beta_0\phi\right)}, \tag{6}$$

[1] The $J(x)$ differs from rapidity by factor $\sqrt{(x+1)/x} = E/Q$, which provides it with correct Q^2-analyticity (see, e.g., Eq. (24.4) in the text [13]).

[2] For a more precise two-loop solution, see Subsec. 2.5 below.

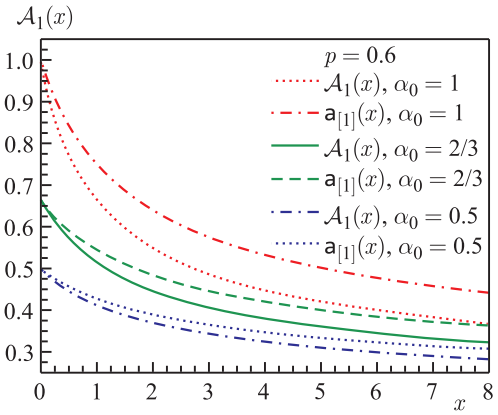

Fig. 3. Quantity $a_{[1]}$ vs. $\mathcal{A}_1(x) = a_{[2]}$

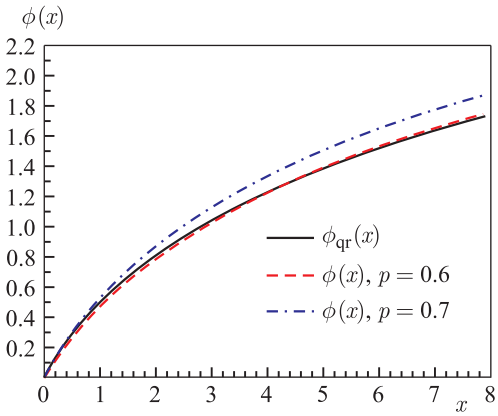

Fig. 4. Quantity $\phi(x)$ vs. $\phi_{\rm qr}(x)$

which corresponds to the perturbation theory expansion in the form

$$\alpha_s(x)^{[2]}_{\rm MPT} = a_{\rm PT}(\phi) = \alpha_0 - \alpha_0^2\beta_0\,\phi(x) + \alpha_0^3\,[\beta_0\phi(x)]^2 - \alpha_0^3\,\beta_1\phi(x), \tag{7}$$

that reflects our *ansatz on the functional equality* of one- and two-loop massive contributions which we take in a simple form

$$\phi = \ln(1 + px). \tag{8}$$

Below, we use the 3-flavor values of coefficients in (7): $\beta_0 = 0.716$, $\beta_1 = 0.405$, $b = \beta_1/\beta_0 = 0.566$.

The 1-loop expression is also of interest:

$$\mathsf{a}(\phi) \lesssim \mathsf{a}_{[1]}(\phi) = \frac{\alpha_0}{1 + \alpha_0\beta_0\phi} \lesssim 1.16\,\mathsf{a}(\phi), \tag{9}$$

with maximum *relative* deviation (see Fig. 3) from $\mathsf{a}_{[2]} = \mathsf{a}\,(\phi)$ at $p\,x_{\max} = e - 1 = 1.72$.

The p parameter can be estimated by comparing $\phi(x)$ (Fig. 4) with the "quasi-rapidity" model:

$$\phi_{\rm qr}(x) = 2\sqrt{\frac{x+1}{x}}\,\ln(\sqrt{x} + \sqrt{x+1}) - 2. \tag{10}$$

This gives for the parameter p the following value: $p \sim 0.60 \pm 0.05$, $\sqrt{x_{\max}} \sim 1.7$. For the α_0 *parameter* assess, one can use the BjSR threshold condition

$$\frac{\alpha_0}{\pi} + 0.363\alpha_0^2 + 0.652\alpha_0^3 + 1.804\alpha_0^4 > 1 \Rightarrow \alpha_0^{\rm PT} \gtrsim 0.69. \tag{11}$$

2.2. Condition on $\mathcal{A}_1(m_\tau)$. The normalization (conjunction) condition

$$\mathcal{A}_1(x_\tau) = 0.330 \pm 0.014, \tag{12}$$

combined with (6), yields a relation, at fixed $p = 0.6$, between two quantities α_0 and $M_{\rm glb}$:

$$X_\tau + b\,\ln X_\tau = 3.03 \pm 0.13 + b\ln\left(\frac{1}{\alpha_0}\right), \tag{13}$$

or in the following form:

$$X_\tau = X_\tau(\alpha_0, M_{\rm glb}) = \frac{1}{\alpha_0} + b\,\ln\left(1 + p\,\frac{m_\tau^2}{M_{\rm glb}^2}\right). \tag{14}$$

Under plausible assumption $\alpha_0 \gtrsim 0.7\,(1/\alpha_0 \lesssim 1.43)$, one gets $X_\tau \gtrsim 2.70$. In turn, this gives $M_{\rm glb} \gtrsim 450$ MeV. For more detailed information, see Figs. 5 and 6. The tendency is simple:

$$\frac{d\,M_{\rm glb}}{d\,\alpha_0} \sim -0.5\ \text{GeV}. \tag{15}$$

However, one has to mind that estimate (11) in the MPT case is under suspicion as it does not account for non-powerness of the MPT expansion. Some more information on $\mathcal{A}_1(x) = a\,(\phi(x))$ can be learnt from Figs. 5 and 6. From there we have

$$M_{\rm glb}(a_0 = 1.0) \sim (512 \pm 43)\ \text{MeV}, \quad M_{\rm glb}(a_0 = 2/3) \sim (661 \pm 61)\ \text{MeV}. \tag{16}$$

To conclude this part, we give the $\mathcal{A}_1$ low-energy behavior vs. common $\bar{\alpha}_s$ and APT A_1 ones, on the one hand (Fig. 7), and vs. lattice simulation results [15] (Fig. 8), on the other hand.

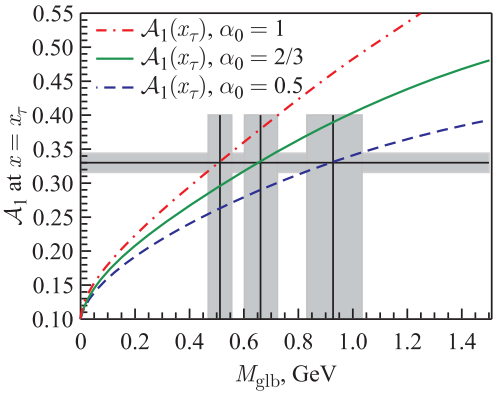

Fig. 5. Parameter $M_{\rm glb}$ estimate vs. three a_0 values

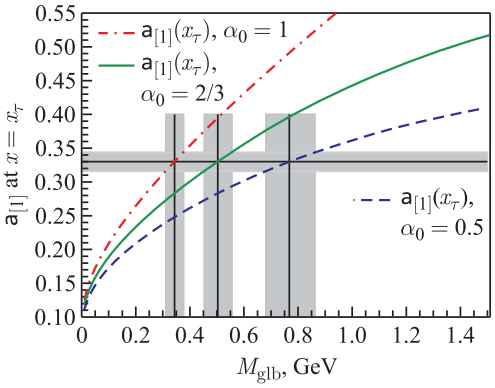

Fig. 6. The same as in Fig. 5 but for the 1-loop case

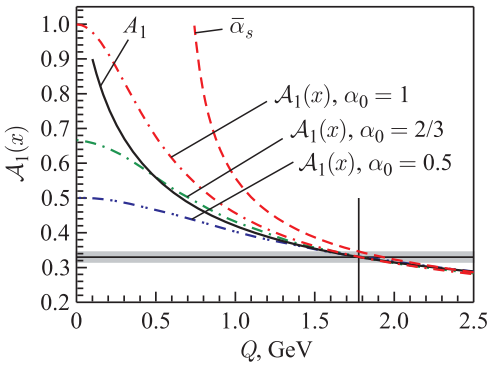

Fig. 7. Various couplings at low-energy domain

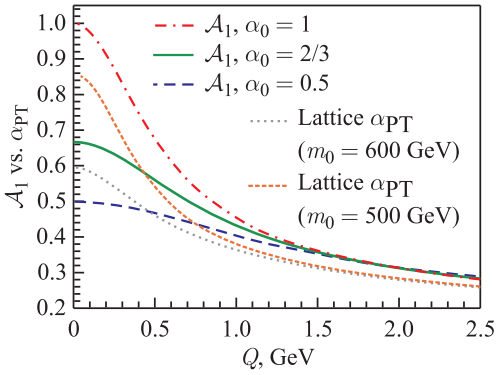

Fig. 8. Quantity $\mathcal{A}_1(Q)$ vs. lattice results [15]

2.3. Recurrent Relation. In the construction under devising, we intend to preserve an essential APT feature, namely, the non-polynomiality of "perturbative" MPT-expansion over a set[1] of functions $\{\mathcal{A}_k(Q^2)\}$.

2.3.1. Differential Recurrency. In the APT, higher functions are connected by the differential recurrent relation

$$-\frac{x}{k}\frac{\partial}{\partial x}\mathcal{A}_k(x) = \beta_0\mathcal{A}_{k+1}(x) + \beta_1\mathcal{A}_{k+2}(x) + \dots \tag{17}$$

To the arguments ascending to the 1980s (see Ref. 11 in [16] and papers [17, 18]) and related to the π^2-term summation procedure in the s-channel (see also [1–5]), one can add a fresher reasoning [19, 20].

This differential recurrency ensures compatibility [21–23] with linear transformations involved in transition to the distance picture (Fourier-conjugated with the momentum-transfer one) and to the annihilation s-channel (reverse Adler transformation).

2.3.2. Comment on Eq. (17). This simple recurrent operator (the log derivative) is an ***ansatz*** *mainly motivated by the structure of π^2-terms [17, 18] generated, in turn, by the UV log branching. Generally, it is an open question how to modify this log-derivative for the mass-dependent structures relevant to the low-energy domain. E.g., one can write instead*

$$-\frac{1}{k}\,\mathfrak{d}_\rho\mathcal{A}_k(x) := \beta_0\mathcal{A}_{k+1}(x) + \beta_1\mathcal{A}_{k+2}(x) + \dots, \quad \mathfrak{d}_\rho = \frac{d}{d\rho(x)}. \tag{18}$$

Here, $\rho(x)$ is an appropriate function, defined for a real positive argument, with log asymptotics.

For the recurrence function, we start with the *simplest* option without additional parameter

$$\rho(x) = \phi(x) - \ln\, p = \ln\,(1 + px) - \ln\, p = \ln\,(x + x_*), \tag{19}$$

where $x = Q^2/M^2_{\rm glb}$ and $x_* = 1/p$. Then, technically

$$\mathfrak{d}_\rho = \mathfrak{d}_\phi :\equiv \mathfrak{d}, \quad \mathfrak{d}\,\mathcal{A}_k(x) = (x + x_*)\mathcal{A}'_k(x), \tag{20}$$

and

$$\mathfrak{d}^2\,\mathcal{A}_k(x) = (x + x_*)^2\mathcal{A}''_k(x) + (x + x_*)\,\mathcal{A}'_k. \tag{21}$$

Our recurrent ansatz

$$\boxed{\beta_0\mathcal{A}_{k+1}(x) = -\frac{1}{k}\,\mathfrak{d}\mathcal{A}_k(x) - \beta_1\mathcal{A}_{k+2}(x), \quad \mathcal{A}_{k\geqslant 5}(x) = 0} \tag{22}$$

leads to three equations for the three expansion functions $\mathcal{A}_{2,3,4}$ in terms of the given $\mathcal{A}_1(x) = \mathsf{a}(\phi)$,

$$\mathcal{A}_2 = -\frac{1}{\beta_0}\,\mathfrak{d}\,\mathsf{a}(\phi) - b\mathcal{A}_3, \quad \mathcal{A}_3 = -\frac{1}{2\beta_0}\mathfrak{d}\mathcal{A}_2 - b\mathcal{A}_4, \quad \mathcal{A}_4 = -\frac{1}{3\beta_0}\mathfrak{d}\mathcal{A}_3. \tag{23}$$

[1] The same symbol $\mathcal{A}$ as in the minimal APT is used.

2.4. Higher SiMPT Functions. Higher Simplest MPT (SiMPT) expansion functions $\mathcal{A}_{2,3,4}$ are defined by Eqs. (23). Their combination yields linear differential equation for $\mathcal{A}_3$ (in the ϕ variable)

$$\mathcal{A}_3(x) = \frac{1}{2\beta_0^2}\,\eth^2\mathsf{a}(\phi) + \frac{5b}{6\beta_0}\,\eth\mathcal{A}_3(x), \quad \eth\mathcal{A}_3 - k\mathcal{A}_3 = -f(\phi), \tag{24}$$

where

$$k = \frac{6\beta_0}{5b} = 1.52, \quad q = \frac{3}{5\beta_1} = 1.48, \quad f(\phi) = q\eth^2\mathsf{a}(\phi). \tag{25}$$

Its solution with AF boundary condition

$$\mathcal{A}_3(x) = a_3(\phi) = q\,\mathrm{e}^{k\phi}\int\limits_{\phi}^{\infty}\eth^2\,\mathsf{a}(f)\,\mathrm{e}^{-kf}\,df = -q\,[\eth\,\mathsf{a}(\phi) + k\,\mathsf{a}(\phi)] + kqI(\phi) \tag{26}$$

contains integral

$$I(\phi) = k\int\limits_{\phi}^{\infty}\mathsf{a}(f)\,\mathrm{e}^{k(\phi-f)}\,df, \tag{27}$$

which is calculated numerically — see Fig. 9 and Table 1. Below, in Figs. 10 and 11, all higher functions $\mathcal{A}_{2,3,4}$ are given numerically via Eqs. (23).

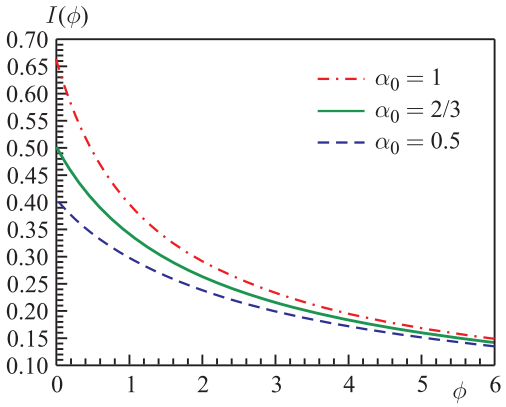

Fig. 9. Integral $I(\phi)$

Table 1. **The values of integral $I(\phi)$ for definite ϕ at fixed parameter α_0**

α_0	ϕ												
	0.0	0.5	1.0	1.5	2.0	2.5	3.0	3.5	4.0	4.5	5.0	5.5	6.0
0.5	0.667	0.492	0.397	0.335	0.292	0.259	0.233	0.213	0.196	0.181	0.169	0.158	0.149
1	0.502	0.404	0.342	0.297	0.263	0.237	0.216	0.198	0.183	0.171	0.160	0.150	0.142
2/3	0.402	0.340	0.296	0.263	0.237	0.218	0.198	0.184	0.171	0.160	0.151	0.142	0.135

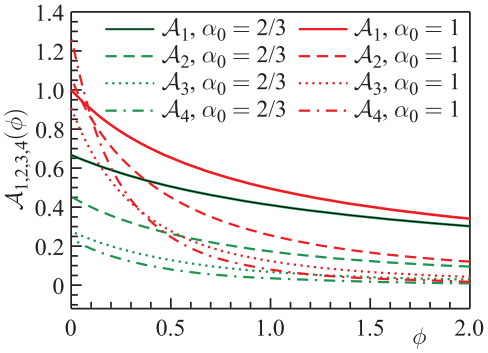

Fig. 10. Functions $\mathcal{A}_{1,2,3,4}(\phi)$ for different values of parameter α_0

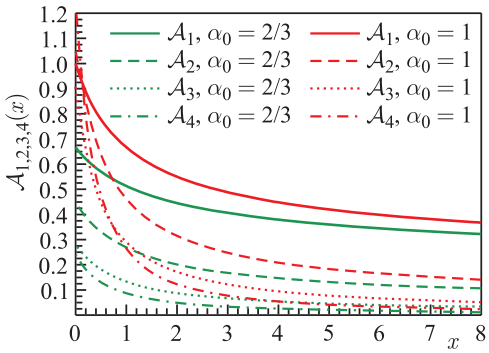

Fig. 11. Functions $\mathcal{A}_{1,2,3,4}(x)$ for different values of parameter α_0

Now, one can verify the preliminary estimate $\alpha_0^{\rm PT} \sim 0.686$, Eq. (11). To this end, on the basis of Tables 2 and 3, we found the perturbation theory sum

$$\Delta_{\rm MPT}(Q) = \sum_k c_k \mathcal{A}_k = \frac{1}{\pi}\mathcal{A}_1 + 0.363\mathcal{A}_2 + 0.652\mathcal{A}_3 + 1.804\mathcal{A}_4, \tag{28}$$

Table 2. **Quantities $\mathcal{A}_{1,2,3,4}$ as functions of ϕ and x**

ϕ	x	$\alpha_0 = 1$					$\alpha_0 = 2/3$				
		Q, GeV	$\mathcal{A}_1$	$\mathcal{A}_2$	$\mathcal{A}_3$	$\mathcal{A}_4$	Q, GeV	$\mathcal{A}_1$	$\mathcal{A}_2$	$\mathcal{A}_3$	$\mathcal{A}_4$
0.00	0.00	0.00	1.000	1.050	0.911	1.289	0.00	0.667	0.454	0.279	0.240
0.15	0.27	0.27	0.858	0.774	0.600	0.717	0.34	0.607	0.377	0.215	0.166
0.25	0.47	0.35	0.786	0.649	0.470	0.509	0.46	0.574	0.337	0.183	0.133
0.50	1.08	0.53	0.653	0.447	0.278	0.245	0.69	0.505	0.261	0.127	0.080
1.00	2.86	0.87	0.495	0.255	0.125	0.080	1.12	0.410	0.172	0.069	0.035
1.25	4.15	1.04	0.443	0.204	0.090	0.051	1.35	0.376	0.144	0.054	0.024
1.50	5.80	1.23	0.402	0.168	0.068	0.034	1.59	0.347	0.123	0.042	0.018
1.70	7.46	1.40	0.375	0.145	0.055	0.026	1.81	0.328	0.109	0.036	0.014

Table 3. **Quantities $\mathcal{A}_{1,2,3,4}$ as functions of Q**

Q, GeV	$\alpha_0 = 1$				$\alpha_0 = 2/3$				$\alpha_0 = 1/2$			
	$\mathcal{A}_1$	$\mathcal{A}_2$	$\mathcal{A}_3$	$\mathcal{A}_4$	$\mathcal{A}_1$	$\mathcal{A}_2$	$\mathcal{A}_3$	$\mathcal{A}_4$	$\mathcal{A}_1$	$\mathcal{A}_2$	$\mathcal{A}_3$	$\mathcal{A}_4$
0.00	1.000	1.050	0.911	1.289	0.66(6)	0.454	0.279	0.239	0.500	0.253	0.120	0.073
0.20	0.911	0.873	0.707	0.904	0.644	0.424	0.253	0.209	0.494	0.247	0.116	0.070
0.40	0.747	0.586	0.408	0.418	0.591	0.357	0.198	0.149	0.477	0.230	0.105	0.061
0.60	0.612	0.392	0.231	0.189	0.530	0.288	0.146	0.097	0.454	0.209	0.091	0.050
0.80	0.519	0.280	0.143	0.097	0.476	0.232	0.107	0.063	0.428	0.186	0.077	0.040
1.00	0.454	0.214	0.097	0.056	0.432	0.191	0.081	0.043	0.404	0.165	0.065	0.031
1.40	0.374	0.145	0.055	0.026	0.369	0.139	0.051	0.023	0.361	0.132	0.047	0.020
1.78	0.330	0.112	0.038	0.015	0.330	0.111	0.037	0.014	0.330	0.110	0.036	0.014

which gives the following values at the infra-red limit:

$$\Delta_{\rm MPT}(Q^2=0;\alpha_0=1)=3.619 \quad \text{and} \quad \Delta_{\rm MPT}(0;\alpha_0=2/3)=0.991. \tag{29}$$

Linear extrapolation gives slightly more accurate bounds

$$\alpha_0^{\rm SiMPT} \lesssim 0.67, \quad M_{\rm glb} \gtrsim 650 \text{ MeV}. \tag{30}$$

The last limitation on $M_{\rm glb}$ does not contradict the current lattice estimate (see review [24]).

2.5. On Exact Two-Loop Massive Solution. The massive renormalization group solution, more precise than (6), is expressible via a special Lambert function $W(z)$.

In this connection, we are reminded that the Lambert function naturally arises in the course of exact solving of the two-loop renormalization group equation for the running coupling in the massless, pure log case. Under simple reservation, the same is true for the massive case.

For this purpose, we analyze massive renormalization group (mRG) solution for the functional equality input. Omitting technical details (see [25,26]), one gets the transcendental relation for $\alpha_s(x)^{[2]}_{\rm mRG}=a(\phi)$:

$$F\left(\alpha_s(x)^{[2]}_{\rm mRG}\right)=F(\alpha_0)+\beta_0\phi(x), \tag{31}$$

$$F(a)=-\beta_0\int^a\frac{da}{\beta(a)}, \quad \beta(a)=\beta_0a^2+\beta_1a^3. \tag{32}$$

If, as usual, the expansion $\beta_0/\beta(a)\sim 1/a^2-b/a$ is used, then

$$F_{\rm ex}(a)=\frac{1}{a}+b\,\ln\,a=V_+(a). \tag{33}$$

Hence,

$$\alpha_s(x)^{[2]}_{\rm mRG,1}=F_1^{-1}\left(F_1(\alpha_0)+\beta_0\,\phi(x)\right). \tag{34}$$

At the same time, a straightforward calculation of the integral in (31) yields

$$F_2(a)=\frac{1}{a}-b\,\ln\left(\frac{1}{a}+b\right):=V_-\left(\frac{1}{a}+b\right)-b \tag{35}$$

and

$$\alpha_s(x)^{[2]}_{\rm mRG,2}=F_2^{-1}\left(F_2(\alpha_0)+\beta_0\,\phi(x)\right). \tag{36}$$

The functions reverse to the just introduced $V_\pm$ are simply related to the Lambert function.

3. LONGITUDINAL AND TRANSVERSE SPIN STRUCTURE AT LOW Q^2

For the purpose of a smooth continuation of $\Gamma_1^{p,n}(Q^2)$ to the non-perturbative region $0\leqslant Q^2\lesssim\Lambda^2_{\rm QCD}$ [27,28], it is convenient to consider the Q^2-evolution of the integral

$$I_1(Q^2)\equiv\frac{2M^2}{Q^2}\Gamma_1(Q^2)=\frac{2M^2}{Q^2}\int\limits_0^1 dx\,g_1(x,Q^2), \tag{37}$$

which is equivalent to the integral over all energies of the spin-dependent photon–nucleon cross section, whose value at $Q^2 = 0$ is defined by the Gerasimov–Drell–Hearn (GDH) sum rule [29, 30]

$$I_1(0) = -\frac{\mu_A^2}{4}, \tag{38}$$

where μ_A is the nucleon anomalous magnetic moment. Then the function $I_1(Q^2)$ can be written as a difference

$$I_1(Q^2) = I_T(Q^2) - I_2(Q^2) \tag{39}$$

between the transverse and "longitudinal minus transverse" structures, where

$$I_T(Q^2) = \frac{2M^2}{Q^2}\Gamma_T(Q^2) \equiv \frac{2M^2}{Q^2}\int\limits_0^1 dx\, g_T(x, Q^2), \tag{40}$$

$$I_2(Q^2) = \frac{2M^2}{Q^2}\int\limits_0^1 dx\, g_2(x, Q^2). \tag{41}$$

The well-known Burkhardt–Cottingham (BC) sum rule [31] provides us with an exact expression for $I_2(Q^2)$, in terms of familiar electric G_E and magnetic G_M Sachs form factors as

$$I_2(Q^2) = \frac{1}{4}\mu G_M(Q^2)\frac{\mu G_M(Q^2) - G_E(Q^2)}{1 + Q^2/4M^2}, \tag{42}$$

where μ is the nucleon magnetic moment. As a consequence of the strong Q^2 behavior of the right-hand side of Eq. (42), we get for large Q^2

$$\int\limits_0^1 g_2(x, Q^2)dx\big|_{Q^2\to\infty} = 0, \tag{43}$$

so I_2 is much smaller than I_1 for large Q^2. Now from the BC sum rule (42), it follows that

$$I_2(0) = \frac{\mu_A^2 + \mu_A e}{4}, \tag{44}$$

where e is the nucleon charge. Then the GDH value (38) is reproduced with

$$I_T(0) = \frac{\mu_A e}{4}. \tag{45}$$

This slope is essentially larger than the one for I_1, explaining the observed excess of the slope of the latter over the GDH value. In practice, as there is currently no evidence that the BC sum rule has any perturbative or non-perturbative corrections, one may apply the SiMPT series to $\Gamma_T(Q^2)$ instead of $\Gamma_1(Q^2)$, which will allow matching to the GDH value.

4. LAMBERT FUNCTION

Generally, the multi-branch Lambert function $W(z)$ of the complex variable z is defined by the relation

$$W(z)\,\mathrm{e}^{W(z)} = z, \quad W(z) + \ln\, W(z) = \ln\, z. \tag{46}$$

One of its asymptotics is

$$W(z)|_{z\to\infty} \to \ln\, z - \ln\,(\ln\, z). \tag{47}$$

Our interest is with a particular branch, $W_{-1}(z)$, real on a real negative semi-axis $-z = t > 1/e$. Farther in this text we shall omit lower index, always having in mind this branch. Then, in the massless case (see [32, 33] and references therein),

$$\alpha_s^{[2]}(Q^2) = -\frac{\beta_0}{\beta_1}\,\frac{1}{1+W(z)}, \quad z = -\exp\left(-\frac{L}{B} - 1\right); \quad L = \ln\left(\frac{Q^2}{\Lambda^2}\right), \quad B = \frac{\beta_1}{\beta_0^2}. \tag{48}$$

According to (47), its asymptotics can be presented as follows:

$$\alpha_s^{[2]}(Q^2) \sim \frac{1}{\beta_0\, L + \beta_1\, \ln L}. \tag{49}$$

In our massive SiMPT case, we can use this expression with the change of the log argument, $L \to \phi(x)$, that is $\ln\, x$ to $\ln\,(x + 1/p)$. For a quantitative estimate, look at the numerical table of Lambert in spirit of Eqs. (8) and (19).

In paper [14], in the course of solving, one meets [1] an equation like

$$\beta_0\phi(x) = J(A(x)) - J(a_0) = -\beta_0 \int\limits_{a_0}^{A_1(x)} \frac{dg}{\beta_0 g^2 + \beta_1 g^3} = -\int\limits_{a_0}^{A_1(\phi(x))} \frac{dg}{g^2 + bg^3}. \tag{50}$$

If the integrand is expanded,

$$\frac{1}{g^2 + bg^3} \simeq \frac{1}{g^2} - \frac{b}{g}, \tag{51}$$

or exact $\beta(g)$ is equal to a formally expanded expression (like in some 2-dim soluble models), then after integration one gets

$$J(A) = \frac{1}{A} + b\,\ln A = b\left(\frac{1}{b\,A} - \ln\frac{1}{b\,A}\right) - b\,\ln b, \tag{52}$$

$$\frac{1}{b}\,(J(A) + b\,\ln b) = \frac{1}{b\,A} - \ln\frac{1}{b\,A}. \tag{53}$$

Exponentiating the last relation, we get

$$\exp\left(\frac{\phi(x)}{B} + \frac{J(a_0)}{b} + \ln b\right) = \exp\left(\frac{J(A)}{b} + \ln b\right) = bA\exp\left(\frac{1}{bA}\right), \tag{54}$$

[1] See p. 31 in our JINR Preprint P2-2008-107, Dubna, 2008 (in Russian).

where $B = \beta_1/\beta_0^2 = 0.790$ and we used (50) to express $J(A)$ in terms of $J(a_0)$. After rearrangement of (54) we get

$$bA \exp\left(\frac{1}{bA}\right) = \exp\left(\frac{\phi(x)}{B} + \frac{1}{ba_0} - \ln\frac{1}{ba_0}\right) = ba_0 \exp\left(\frac{\phi(x)}{B} + \frac{1}{ba_0}\right), \qquad (55)$$

and, using the definition of the Lambert function $W(z)$ (i.e., $W(z)\,\mathrm{e}^{W(z)} = z$), we can write the result as

$$bA(x) = -\left[W\left(-\frac{1}{ba_0}\exp\left(-\frac{\phi(x)}{B} - \frac{1}{ba_0}\right)\right)\right]^{-1}. \qquad (56)$$

If not expanded, it is still calculable and expressible (a bit differently!) via the W Lambert function

$$\frac{1}{g^2 + bg^3} = \frac{1}{g^2} - \frac{b}{g} + \frac{b^2}{1+bg}, \qquad (57)$$

and

$$J_2(A) = \frac{1}{A} - b\,\ln\left(\frac{1}{A} + b\right) = b\left(\frac{1}{bA} + 1 - \ln\left(\frac{1}{bA} + 1\right)\right) - b\,(1 + \ln b). \qquad (58)$$

Again after exponentiation we get

$$\exp\left(\frac{\phi(x)}{B} + \frac{J_2(a_0)}{b} + 1 + \ln b\right) = \exp\left(\frac{J_2(A)}{b} + 1 + \ln b\right) = \frac{\mathrm{e}^{1/(bA)+1}}{1/(bA)+1}. \qquad (59)$$

And the solution is the following:

$$bA(x) = -\frac{1}{W\left[-\dfrac{1+b\,a_0}{ba_0}\,\exp\left(\dfrac{-\phi(x)}{B} - \dfrac{1}{ba_0} - 1\right)\right] + 1}. \qquad (60)$$

The difference between the two expressions:

$$A_1(x) = -\frac{1}{b\,W\left[-\dfrac{1}{ba_0}\exp\left(\dfrac{-\phi(x)}{B} - \dfrac{1}{ba_0}\right)\right]}, \qquad (61)$$

$$A_2(x) = -\frac{1}{b\left\{W\left[-\dfrac{1+ba_0}{ba_0}\exp\left(-\dfrac{\phi(x)}{B} - \dfrac{1}{ba_0} - 1\right)\right]\right\}} \qquad (62)$$

could be essential when the cubical term in $\beta(g)$ is a leading one. This can happen in the low-energy region at $a_0 \sim 1$. There, the difference $A_2(x) - A_1(x)$ is positive and could reach several tenths.

5. OUTLOOK: ON 3-LOOP LONG-LOG

One more way to realize the accuracy of SiMPT is to estimate the possible influence of three-loop effects. This can be done with a specific trick proposed in [34]:

$$L \to L^* = L + B\,\sqrt{L^2 + 2\,\pi^2}. \qquad (63)$$

Acknowledgements. It is our pleasure to thank Yu. M. Bystritskiy for useful advice and technical help. This research has been partially supported by the JINR–BelRFFR grant F14D-007 and by the RFBR grant 14-01-00647.

The manuscript was prepared for publication with the participation of P. Fiziev, O. V. Teryaev, S. V. Mikhailov, O. P. Solovtsova, and Yu. M. Bystritskiy.

REFERENCES

1. *Shirkov D. V., Mikhailov S. V.* Mass Dependent α_s Evolution and the Light Gluino Existence // Z. Phys. C. 1994. V. 63. P. 463.
2. *Simonov Yu. A.* Perturbative Theory in the Nonperturbative QCD Vacuum // Phys. At. Nucl. 1995. V. 58. P. 107.
3. *Badalian A. M., Simonov Yu. A.* Freezing of $\alpha_s(Q^2)$ in e^+e^- Annihilation // Phys. At. Nucl. 1997. V. 60. P. 630.
4. *Shirkov D. V., Sidorov A. V., Mikhailov S. V.* Continuous Mass Dependent Analysis of the Nonsinglet xF_3 CCFR Data. arXiv:hep-ph/9707514.
5. *Nesterenko A. V., Papavassiliou J.* A Novel Integral Representation for the Adler Function // J. Phys. G. 2006. V. 32. P. 1025.
6. *Shirkov D. V., Solovtsov I. L.* Analytic Model for the QCD Running Coupling with Universal $\bar{\alpha}_s(0)$ Value // Phys. Rev. Lett. 1997. V. 79. P. 1209.
7. *Solovtsov I. L., Shirkov D. V.* Analytic Approach in Quantum Chromodynamics // Theor. Math. Phys. 1999. V. 120. P. 1220.
8. *Shirkov D. V., Solovtsov I. L.* Ten Years of the Analytic Perturbation Theory in QCD // Theor. Math. Phys. 2007. V. 150. P. 132.
9. *Khandramai V. L. et al.* Four-Loop QCD Analysis of the Bjorken Sum Rule vs Data // Phys. Lett. B. 2012. V. 706. P. 340.
10. *Shirkov D. V.* "Massive" Perturbative QCD, Regular in the IR Limit // Phys. Part. Nucl. Lett. 2013. V. 10. P. 186.
11. *Lipatov L. N.* Quark Scattering Amplitudes with Quasielastic Unitarity // Nucl. Phys. B. 1988. V. 309. P. 379.
12. *Shirkov D. V.* The Unitary Mechanism of Infrared Freezing in QCD with Massive Gluons // Phys. At. Nucl. 1999. V. 62. P. 1928.
13. *Bogolyubov N. N., Shirkov D. V.* Quantum Fields. USA: Benjamin/Cummings, 1983. 388 p.
14. *Shirkov D. V.* Mass Dependences in Renormalization-Group Solutions // Theor. Math. Phys. 1982. V. 49. P. 1039.
15. *Aguilar A. C. et al.* Non-Perturbative Comparison of QCD Effective Charges // Phys. Rev. D. 2009. V. 80. P. 085018.
16. *Radyushkin A. V.* Optimized Λ-Parametrization for the QCD Running Coupling Constant in Space-Like and Time-Like Regions // JINR Rapid Commun. 1996. No. 78. P. 96.
17. *Krasnikov N. V., Pivovarov A. A.* The Influence of the Analytical Continuation Effects on the Value of the QCD Scale Parameter Lambda Extracted from the Data on Charmonium and Upsilon Hadron Decays // Phys. Lett. B. 1982. V. 116. P. 168.
18. *Jones H. F., Solovtsov I. L.* QCD Running Coupling Constant in the Timelike Region // Phys. Lett. B. 1995. V. 349. P. 519.
19. *Shirkov D. V.* Renorm-Group, Causality and Nonpower Perturbation Expansion in QFT // Theor. Math. Phys. 1999. V. 119. P. 438.

20. *Shirkov D. V.* Nonpower "Spectral" Perturbation Expansion in QFT // Lett. Math. Phys. 1999. V. 48. P. 135.
21. *Shirkov D. V.* Analytic Perturbation Theory for QCD Observables // Theor. Math. Phys. 2001. V. 127. P. 409.
22. *Shirkov D. V.* On the Fourier Transformation of Renormalization Invariant Coupling // Theor. Math. Phys. 2003. V. 136. P. 893.
23. *Shirkov D. V.* Nonpower Expansions for QCD Observables at Low Energies // Nucl. Phys. Proc. Suppl. 2006. V. 152. P. 51.
24. *Ochs W.* The Status of Glueballs // J. Phys. G. 2013. V. 40. P. 043001.
25. *Shirkov D. V.* Perturbative Analysis of General Renorm Group Solutions in a Massive Case // Nucl. Phys. B. 1992. V. 371. P. 467.
26. *Shirkov D. V.* Mass and Scheme Effects in Coupling Constant Evolution // Theor. Math. Phys. 1992. V. 93. P. 1403.
27. *Soffer J., Teryaev O. V.* The Role of $g - 2$ in Relating the Schwinger and Gerasimov–Drell–Hearn Sum Rules // Phys. Rev. Lett. 1993. V. 70. P. 3373.
28. *Soffer J., Teryaev O. V.* QCD Radiative and Power Corrections and Generalized GDH Sum Rules // Phys. Rev. D. 2004. V. 70. P. 116004.
29. *Gerasimov S. B.* A Sum Rule for Magnetic Moments and the Damping of the Nucleon Magnetic Moment in Nuclei // Sov. J. Nucl. Phys. 1966. V. 2. P. 430.
30. *Drell S. D., Hearn A. C.* Exact Sum Rule for Nucleon Magnetic Moments // Phys. Rev. Lett. 1966. V. 16. P. 908.
31. *Burkhardt H., Cottingham W. N.* Sum Rules for Forward Virtual Compton Scattering // Ann. Phys. 1970. V. 56. P. 453.
32. *Magradze B. A.* The Gluon Propagator in Analytic Perturbation Theory // Conf. Proc. C. 1999. V. 980518. P. 158.
33. *Magradze B. A.* A Novel Series Solution to the Renormalization Group Equation in QCD // Few Body Syst. 2006. V. 40. P. 71.
34. *Shirkov D. V., Zayakin A. V.* Analytic Perturbation Theory for Practitioners and Upsilon Decay // Phys. At. Nucl. 2007. V. 70. P. 775.

Received on October 24, 2014.